

PAPER

Room-Temperature Organic Negative Differential Resistance Device Using CdSe Quantum Dots as the ITO Modification Layer_*

To cite this article: Bo Jiao et al 2015 Chinese Phys. Lett. 32 117301

View the article online for updates and enhancements.

You may also like

- Evaluating the Roles of Proton Transfer and H-Bonding in the Electron Transfer Reactions of Organic Redox Couples in Non-Aqueous Solvents: Oxidation of Phenylenediamines in the Presence of Added Bases in Acetonitrile Tammy Dung Pham and Diane K. Smith
- <u>Spatiotemporal Patterns Formed on p-Type Silicon Electrodes during Electrochemical Dissolution</u> Yuya Suzuki, Tomoko Urata, Kazuhiro Fukami et al.
- Analysis of Thermal Degradation in Oxide <u>Thin Film Transistors</u>
 Yukiharu Uraoka, Satoshi Urakawa and Yasuaki Ishikawa

Room-Temperature Organic Negative Differential Resistance Device Using CdSe Quantum Dots as the ITO Modification Layer *

JIAO Bo(焦博)¹, YAO Li-Juan(姚丽娟)¹, WU Chun-Fang(吴春芳)², DONG Hua(董化)¹, HOU Xun(侯洵)¹, WU Zhao-Xin(吴朝新)^{1**}

¹Key Laboratory for Physical Electronics and Devices of the Ministry of Education & Shannxi Key Lab of Information Photonic Technique, School of Electronic and Information Engineering, Xi'an Jiaotong University, Xi'an 710049 ²School of Physical Science and Technology, Lanzhou University, Lanzhou 730000

(Received 17 August 2015)

Room-temperature negative differential resistance (NDR) has been observed in different types of organic materials. However, detailed study on the influence of the organic material on NDR performance is still scarce. In this work, room-temperature NDR is observed when CdSe quantum dot (QD) modified ITO is used as the electrode. Furthermore, material dependence of the NDR performance is observed by selecting materials with different charge transporting properties as the active layer, respectively. A peak-to-valley current ratio up to 9 is observed. It is demonstrated that the injection barrier between ITO and the organic active layer plays a decisive role for the device NDR performance. The influence of the aggregation state of CdSe QDs on the NDR performance is also studied, which indicates that the NDR is caused by the resonant tunneling process in the ITO/CdSe QD/organic active layer structure.

PACS: 73.21.La, 72.80.Le, 74.50.+r DOI: 10.1088/0256-307X/32/11/117301

Negative differential resistance (NDR) devices have attracted considerable attention due to their enormous potential application in nonvolatile memory, low power logic circuits, oscillators, etc. [1] Recently, NDR phenomena have been observed in different structures based on organic materials, [2-9] such as superlattice structure, [2,4] dye-doped OLEDs[3] and nanoparticle-organic hybrid structures.[5-9] Typically. these NDR phenomena can be observed at room temperature, which indicates their great potential for real application. However, there are still many problems to be solved. Firstly, although NDR phenomena have been observed in different types of materials, including polymer and small molecular, the relationship between the NDR phenomenon and the property of the organic material is still unclear. Secondly, the origin of the NDR phenomenon is still a disputed issue. For example, Tang et al.[10] believed that the NDR phenomenon is derived from the blockade of mobile charge carriers by the internal space-charge field that is created by the trapped charges, which is also referred to as the Coulomb blockade mechanism. [11,12] Gorman et al. [13] elucidated the NDR phenomenon in microscopic organic NDR devices by the resonant tunneling mechanism. Furthermore, Berleb $et \ al.^{[14]}$ ascribed the spatially localized current pathways to the organic NDR phenomenon at low voltage.

Recently, semiconductor quantum dot (QD) organic hybrid structures have been demonstrated as an effective way to build the NDR device. For example, Yang et al. observed the NDR phenomenon

from CdSe/ZnS core-shell colloidal QDs-based organic light-emitting diodes, [9] Kannan et al. reported the NDR phenomenon with large peak-to-valley current ratio (PVCR) in CdSe QDs/MEH-PPV multilayer heterostructures. [7,8] However, detail description about the influence of an organic active layer as well as the morphology of the QD layer on device NDR performance is still scarce. In this Letter, room-temperature NDR has been observed in a device by using ITO surface modified by CdSe QDs. Furthermore, the influence of the morphology of the CdSe QD layer on the NDR performance is studied and the origin of the NDR phenomenon of these devices is also discussed.

In this study, CdSe nanocrystal QDs with capping ligand tri-n-octylphosphine oxide (TOPO), as shown in the inset of Fig. 1, were synthesized according to the procedure developed by Qu et al., [15] and were dispersed in chloroform. As shown in Fig. 1, the transmission electron microscope (TEM) test demonstrated that the size of the CdSe QDs is around 4 nm. As shown in the inset of Fig. 1, the characteristic peak of CdSe QDs around 580 nm can be observed in its absorption spectrum. The mole concentration of CdSe QDs can be evaluated from the absorption spectrum according to Lambert-Beer's Law and the extinction coefficient of CdSe. [16] The CdSe QD modification layer was spin-coated on ITO glass with sheet resistance of 25Ω . The spin speed for CdSe QD solutions with different concentrations is fixed at 1000 rpm. Then, the CdSe QD layer was annealed at 80°C for 30 min in a vacuum oven. After the CdSe

^{*}Supported by the National Natural Science Foundation of China under Grant Nos 61106123 and 61275034, and the National Basic Research Program of China under Grant No 2013CB328705.

^{**}Corresponding author. Email: zhaoxinwu@mail.xjtu.edu.cn

^{© 2015} Chinese Physical Society and IOP Publishing Ltd

QDs-modified ITO substrate cooling, the organic layer and the aluminum cathode were fabricated by thermal evaporation in a vacuum of 1×10^{-3} Pa. The device fabrication and test process are the same as our previous report. [17] For each structure, at least 12 devices were fabricated and tested. The effective area of these devices is around $12 \,\mathrm{mm}^2$. All of the tests are carried out in air atmosphere and room temperature.

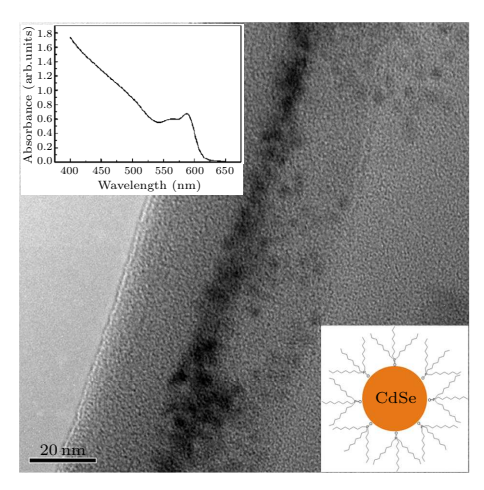


Fig. 1. The TEM photograph of the CdSe QDs. The absorption spectrum of CdSe QDs in chloroform solution and the molecular structure of CdSe QD are shown in the insets, respectively.

Device with the structure of ITO/CdSe QDs/organic active layer (60 nm)/N,N'-biphenyl-N,N'-bis(1-naphthyl)-(1,1'-biphenyl)-4,4'-diamine(NPB) (40 nm)/Al (100 nm) was fabricated to demonstrate the NDR. A 40-nm thick NPB layer was used as the electron-blocking layer to exclude the influence of electrons that were injected from the aluminum cathode on the NDR performance. [18] The CdSe QD concentration for this modification layer is 8 nmol/L. Three different organic materials, including tris(8-hydroxy-quinolinato) aluminum (Alq₃), 4,4'bis(carbazol-9-yl) biphenyl (CBP), and NPB, were selected as the active layer to examine the influence of carrier transport property of the organic active layer on the NDR phenomenon. Here Alq₃, CBP and NPB are representatives of electron transporting material, [19] bipolar transporting material, [20] and hole transporting material, [21] respectively. Control devices without the CdSe QD modification layer were also fabricated. In the fabrication of control devices, ITO surfaces were spin-coated with pure chloroform solvent and then annealing at 80°C for 30 min in a vacuum oven to exclude the probable influence of the solvent as well as the annealing process on the device performance.

Typical current-voltage (I-V) characteristics of devices mentioned above are shown in Fig. 2. As shown in Fig. 2(a), when the Alq₃ and CBP were used as the active layer respectively, NDR phenomena can be observed not in all control devices while in CdSe

QDs-modified devices. It is also found that the conduction current of NDR device is higher than that of the control device at the same voltage. Since the electron injection from the cathode is blocked by the NPB layer, a higher current indicates that this CdSe QD layer can enhance the hole injection from the ITO anode. When NPB is used as the active layer, however, no NDR phenomenon can be observed in both the CdSe QD-modified device and the control device. Furthermore, as shown in Fig. 2(b), use of the CdSe QD layer will decrease the conduction current of the device. Compared with the Alq₃ and the CBP active layers, the NPB layer exhibits two particular characteristics: one is its strong single-carrier (hole) transporting property. The hole mobility of NPB is significantly stronger than its electron mobility. [22,23] The other is the low injection barrier between ITO and the highest occupied molecular orbital (HOMO) of NPB, as shown in the inset of Fig. 2(b), the barriers at interfaces of ITO/Alq₃, ITO/CBP, and ITO/NPB are about 0.9 eV, 1.2 eV, and 0.5 eV, respectively.

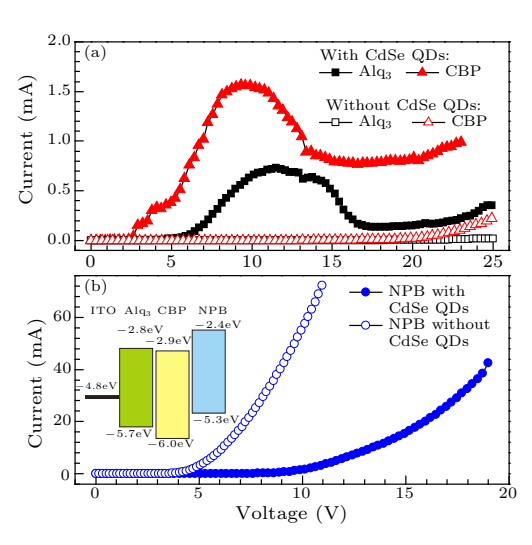


Fig. 2. Typical I-V characteristics of CdSe QDs-modified devices and corresponding control device by using (a) Alq₃, CBP and (b) NPB as the active layer, respectively. The diagrams of energy levels of ITO, Alq₃, CBP, and NPB are also shown in the inset of (b).

To understand the key factor that induces the material dependence of NDR, two additional materials, 4,4',4"-Tris(carbazol-9-yl) triphenylamine (TcTa) and 4,4',4"-Tris (N-3-methylphenyl-N-phenyl-amino) triphenylamine (m-MTDATA), are selected as the organic active layer, respectively. Both TcTa and m-MTDATA exhibit strong hole transporting property.^[24,25] However, the injection barrier at ITO/TcTa interface ($\sim 0.9 \, \text{eV}$) is much larger than that at ITO/m-MTDATA interface ($\sim 0.4 \, \text{eV}$) (see the inset of Fig. 3). As shown in Fig. 3, it can be found that, for the device based on TcTa, use of the CdSe QD layer can increase the conduction current and a significant NDR can be observed. However, as shown in the inset of Fig. 3, for the device based on m-MTDATA,

the CdSe QD layer decreases the conduction current significantly, and no NDR phenomenon can be observed in all the fabricated samples. Thus it can be deduced that the injection barrier at interface of the ITO/active layer is crucial for the NDR performance.

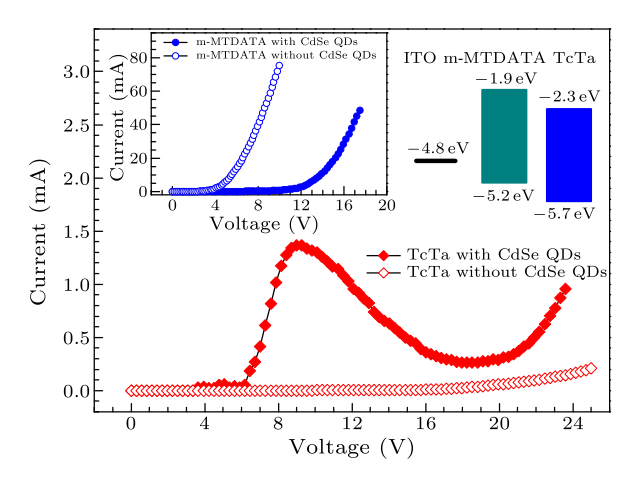


Fig. 3. Typical I-V characteristics of CdSe QD-modified devices and the corresponding control device using TcTa and m-MTDATA (inset) as the active layer, respectively. The diagrams of energy levels of ITO, TcTa and m-MTDATA are also shown.

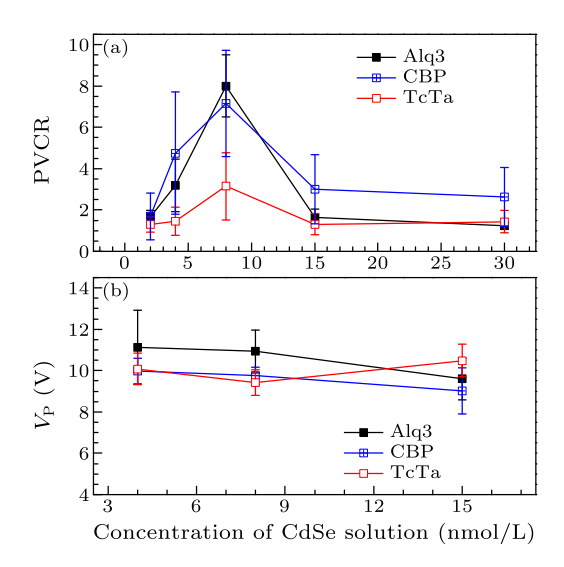


Fig. 4. The PVCR (a) and $V_{\rm p}$ (b) of NDR devices versus concentration of CdSe QD solution.

PVCR is an important index for the performance of NDR devices. In this work, the dependence of PVCR of the NDR device on the morphology of the CdSe QD layer is also studied. Since the spin speed for CdSe QD solutions with different concentrations is a fixed value, the morphology of CdSe QD modification layer is only affected by the solution concentration. As in the description of previous reports, [7,9,10] many factors can affect the NDR phenomenon such as the scanning direction as well as the number that the scanning runs. Here the I-V characteristics of those NDR devices are all measured from $0\,\mathrm{V}$ to $25\,\mathrm{V}$, and only the PVCR of the first sweep is recorded for statistics.

As shown in Fig. 4(a), when the concentration of CdSe QD solution varies from 2 nmol/L to 30 nmol/L, the average PVCR increases first and then decreases. The optimal concentration for the highest PVCR is around 8 nmol/L.

Peak voltage (V_p) , which is a voltage point that the slope of the I-V curve changes from a positive value to a negative value, is a parameter which is important for NDR applications. The dependence of V_p on the organic active material as well as the surface morphology are shown in Fig. 4(b). In our test, the V_p value differs from one device to another and ranges from 7 V to 13 V, which echoes the previous report. [7–9] As shown in Fig. 4(b), statistical results reveal that the influence of the material type and the surface morphology on the V_p is limited, which may indicate that the mechanism that induces the NDR phenomenon is almost the same for NDR devices based on different materials and different surface morphologies.

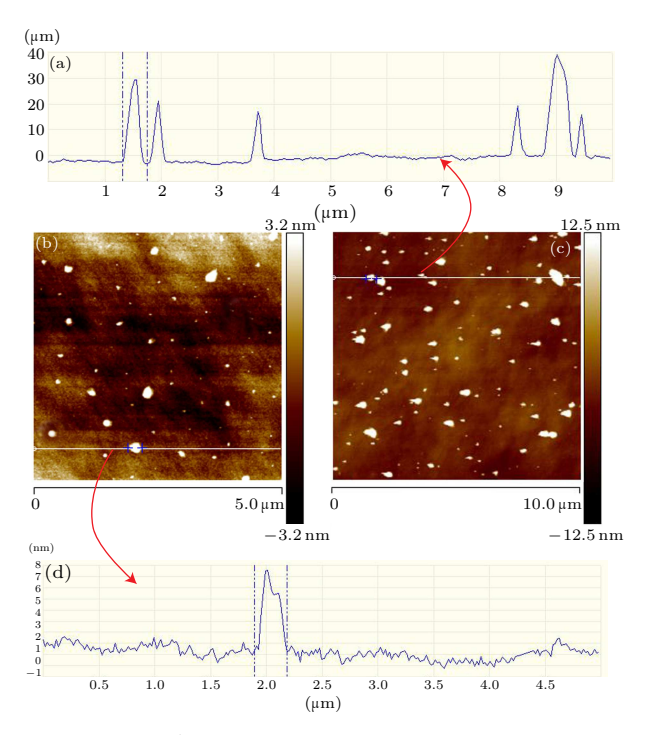


Fig. 5. The AFM morphologies of the CdSe QDs modification layer on the Si layer fabricated by solutions with 8 nmol/L (b) and 30 nmol/L (c), respectively. Height images of the CdSe QD layer along the line section in (b) and (c) are shown in (a) and (d), respectively.

The AFM morphology of the CdSe QD layer fabricated by solutions with 8 nmol/L and 30 nmol/L are shown in Figs. 5(b) and 5(c), respectively. As shown in Figs. 5(b) and 5(c), due to the fact that the concentration of solution used in this study is rather small, CdSe QD layers fabricated by these two solutions all exhibit island morphologies. As shown in Fig. 5(a), the height of islands fabricated by the 8 nmol/L CdSe QDs solution is around 5 nm, which means that the CdSe island is formed by nearly a single monolayer of CdSe QDs. However, as shown in Fig. 5(d), the height

of islands fabricated by the 30 nmol/L CdSe QD solution is around 20 nm, which means that, in the direction perpendicular to the surface, nearly four or more of CdSe QDs are aggregated to form an island.

The influence of CdSe QD aggregation on the device PVCR provides a clue to understand the origin of the NDR phenomenon as well as that of the material dependence. The spatially localized current pathway mechanism^[14] can be excluded since the CdSe layer is too thin (<30 nm) to form a localized pathway compared with the thickness of the organic layer (~60 nm). Furthermore, the Coulomb blockade mechanism^[10] can also be excluded. According to the Coulomb blockade mechanism, the charge will be trapped in CdSe QDs. Thus a higher CdSe QD aggregation degree will benefit the capture of carriers, which will enhance the NDR phenomenon, i.e., the PVCR value will increase. However, as shown in Fig. 4(a), with the increase of the CdSe QD concentration, i.e., the increase of the QDs aggregation state, the PVCR value decreases dramatically.

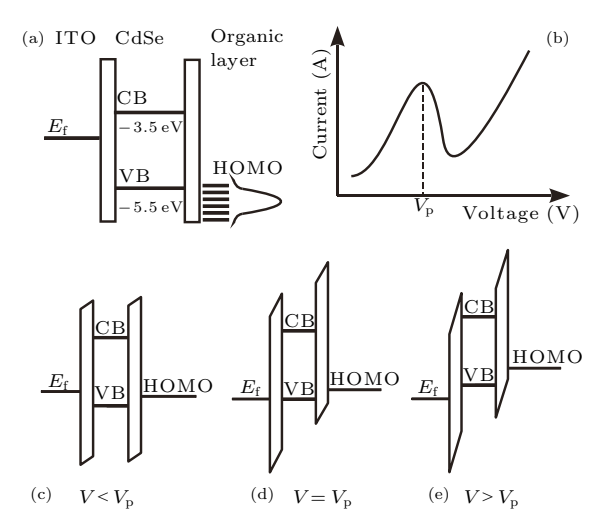


Fig. 6. The diagrams of energy level of ITO/CdSe QD/organic layer structure (a) and a typical NDR I-V curve (b). The arrangement of energy levels at different voltages are shown in (c), (d), and (e) respectively.

Resonant tunneling mechanism^[13] can provide an appropriate understanding for the NDR phenomenon of the CdSe QD-based device. The TOPO capped CdSe QDs can be considered as an ideal doublebarrier and single potential well structure, as shown in Fig. 6(a). As mentioned above, there is a peak voltage $(V_{\rm p})$ in a typical NDR I-V curve. As shown in Fig. 6(b), V_p is a turning point at which the slope of the I-V curve changes from a positive value to a negative value. According to the resonant tunneling mechanism, this process can be understood as follows: with the increase of the applied voltage, the overlap between the Fermi level (E_f) of ITO, the valence band (VB) of CdSe QDs and the HOMO of the organic layer approaches a resonance state, as shown in Fig. 6(c), which indicates that the hole injection from the ITO

to the organic layer is enhanced. Thus the conduction current increases. When the applied voltage increases to $V_{\rm p}$, the system achieves the optimal resonance state, as shown in Fig. 6(d), and the conduction current is the maximum. When the applied voltage increases further, the resonance is broken due to the mismatch between the Fermi level of ITO and the VB of CdSe QDs, just as shown in Fig. 6(e), and the hole injection at ITO interface is suppressed dramatically. Thus the conduction current decreases significantly. As can be seen from Fig. 6(a), the VB of CdSe QDs ($\sim -5.5 \, \text{eV}$) is lower than the HOMO of the organic active material used in this study, i.e., Alq₃ (-5.7 eV), TcTa (-5.7 eV)and CBP(-6.0 eV). In the analogous situation of the inorganic NDR device with double-barrier and single potential well structure, the resonant tunneling current should be rather small due to the high electronic energy level of charge collector. [26] However, for the situation of the organic material, the HOMO states of the organic semiconductor material are subject to a Gaussian distribution of energies.^[27] Thus just as shown in Fig. 6(a), partial HOMO states which are lower than the VB of CdSe QDs will take part in the resonant tunneling process and will enhance the carrier injection from ITO anode to the organic layer.

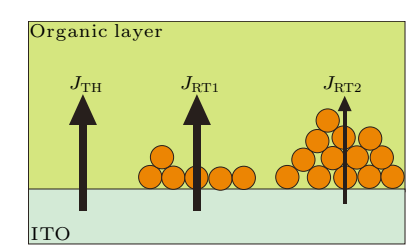


Fig. 7. Schematic diagram of the hole injection channel from ITO to the organic layer.

The morphology-dependent phenomenon can also be ascribed to the influence of CdSe QD aggregation state on the resonant tunneling process. Just as shown in Fig. 5, CdSe QDs aggregate randomly in the spincoating process. This random aggregation disturbs the overlap of the electronic energy level of aggregated CdSe QDs, which will significantly suppress the formation of a resonant tunneling state within the aggregated CdSe QD system. Thus just as shown in Fig. 7, the resonant tunneling current (J_{RT1}) through the CdSe QD monolayer is much larger than the resonant tunneling current (J_{RT2}) through the aggregated CdSe QD multilayer, which makes the NDR performance decrease dramatically with the increase of CdSe QD aggregation degree. Furthermore, the material-dependent phenomenon can also be understood by the resonant tunneling process. As shown in Fig. 7, the discontinuous nature of the CdSe QD modification layer indicates that the total injection current J can be expressed as $J = J_{TH} + J_{RT}$, where J_{RT} is the resonant tunneling current injected from the ITO/CdSe QD/organic layer structure, $J_{\rm TH}$ is the thermionic emission current injected from the ITO/organic layer interface. Here $J_{\rm TH}$ can be described by the Richardson–Schottky equation $J_{\rm TH} \propto$ $T^2 \exp(-\varphi/kT)$, where T is the temperature, and ϕ is the injection barrier.^[28] Thus for the device with smaller ITO/organic injection barrier, such as devices based on NPB and m-MTDATA, the thermionic emission injection process dominates the injection process, and the NDR phenomenon is hard to observe. Moreover, CdSe QD islands work as obstacles for the thermionic emission injection process, which will decrease the injection area, and thus leads to the decrease of the conduction current. However, for the device with large ITO/organic injection barrier, such as devices based on Alq₃, CBP, and TcTa, significant NDR can be observed due to the fact that the thermionic emission injection process is significantly suppressed by the large injection barrier at ITO/organic interface.

In conclusion, room-temperature NDR devices using CdSe QD modified ITO as the anode and organic small molecules as the active layer have been demonstrated. It is found that the key factor that determines the room-temperature NDR phenomenon is not the carrier transport property but the carrier injection barrier between the ITO and the organic active layer. The resonant tunneling mechanism is used to explain the origin of the NDR phenomenon. Our study provides a detailed understanding of the QDs-based organic NDR device and will benefit the design and performance optimization of NDR devices.

References

- Chang L L, Esaki L and Tsu R 1974 Appl. Phys. Lett. 24 593
- [2] Park T J, Lee Y K, Kwon S K, Kwon J H and Jang J 2006 Appl. Phys. Lett. 89 151114
- [3] Xu X H, Han M C and Yin S G 2003 Chin. J. Lumin. 24 459

- [4] Wang Z, Wang T, Wang H B and Yan D H 2014 Adv. Mater. 26 4582
- [5] Zheng T, Choy W C H and Sun Y 2009 Adv. Funct. Mater. 19 2648
- [6] Zheng T, Choy W C H and Sun Y 2009 Appl. Phys. Lett. 94 123303
- [7] Kannan V, Rajesh K R, Kim M R, Chae Y S and Rhee J K 2011 Appl. Phys. A 102 611
- [8] Kannan V, Kim M R, Chae Y S, Ramana C V V and Rhee J K 2011 Nanotechnology 22 025705
- [9] Yang S, Liu P, Guo S, Zhang L, Yang D, Jiang Y and Zou B 2014 Appl. Phys. Lett. 104 033301
- [10] Tang W, Shi H Z, Xu G, Ong B S, Popovic Z D, Deng J C, Zhao J and Rao G H 2005 Adv. Mater. 17 2307
- [11] Shin M, Lee S, Park K W and Lee E H 1998 $Phys.\ Rev.\ Lett.\ {\bf 80}\ 5774$
- [12] Shin M, Lee S, Park K W and Lee E H 1999 Phys. Rev. B 59 3160
- [13] Gorman C B, Carroll R L and Fuierer R R 2001 Langmuir 17 6923
- [14] Berleb S, Brütting W and Schwoerer M 1999 Synth. Met. 102 1034
- [15] Qu L and Peng X 2002 J. Am. Chem. Soc. 124 2049
- [16] Yu W W, Qu L, Guo W and Peng X 2003 Chem. Mater. 15 2854
- [17] Jiao B, Zhu X B, Wu Z X, Yu Y and Hou X 2014 Chin. Phys. Lett. 31 097801
- [18] Zhang S T, Wang Z J, Zhao J M, Zhan Y Q, Wu Y, Zhou Y C, Ding X M and Hou X Y 2004 Appl. Phys. Lett. 84 2916
- [19] Barth S, Müller P, Riel H, Seidler P F, Rieß W, Vestweber H and B ässler H 2001 J. Appl. Phys. 89 3711
- [20] Chen P, Xie W F, Li J Guan T, Duan Y, Zhao Y, Liu S Y, Ma C S, Zhang L Y and Li B 2007 Appl. Phys. Lett. 91 073511
- [21] Jiao B, Wu Z X, Yan X W and Hou X 2010 Appl. Phys. A 98 239
- [22] Tse S C, Kwok K C and So S K 2006 Appl. Phys. Lett. $\bf 89$ 262102
- [23] Deng Z B, Lee S T, Webb D P, Chan Y C and Gambling W A 1999 Synth. Met. 107 107
- [24] Shirota Y, Kuwabara Y, Inada H, Wakimoto T, Nakada H, Yonemoto Y, Kawami S and Imai K 1994 Appl. Phys. Lett. 65 807
- [25] Noh S, Suman C K, Hong Y and Lee C 2009 J. Appl. Phys. 105 033709
- [26] Dakhlaoui H 2013 Chin. Phys. Lett. 30 077304
- [27] Bassler H 1993 Phys. Status Solidi B **175** 15
- [28] Simmons J G 1965 Phys. Rev. Lett. 15 967